

Hadronic Trigger using electromagnetic calorimeter and particle identification at high- p_T with the STAR Detector

Hongyu Da ^a, Xiangli Cui ^{a,b}, Gene Van Buren ^b, J.C. Dunlop ^b,
 Xin Dong ^c, Lijuan Ruan ^b, Anthony Timmins ^d, Zebo Tang ^a,
 Xiaolian Wang ^a, Yichun Xu ^a, Zhangbu Xu ^b

^a*Department of Modern Physics, University of Science and Technology of China, Hefei, Anhui, China, 230026*

^b*Department of Physics, Brookhaven National Laboratory, Upton, NY 11973, USA*

^c*Lawrence Berkeley National Laboratory, 1 Cyclotron Road, Berkeley, CA 94720, USA*

^d*Physics Department, 617 Science & Research Building 1, Houston, TX 77204*

Abstract

We derive a new method to improve the statistics of identified particles at high transverse momentum (p_T) using online-triggered events by the STAR Barrel Electro-Magnetic-Calorimeter (BEMC) detector. The BEMC is used to select charged hadrons (π^\pm , K^\pm and $p(\bar{p})$) via hadronic shower energy deposited in the BEMC. With this trigger, the statistics of the high p_T particles are significantly enhanced (by a factor of up to ~ 100 for STAR) with trigger efficiency up to 20%. In addition, resonant states (ρ^0 , K^*) and weak-decay V0s (K_S^0 and $\Lambda(\bar{\Lambda})$) can be constructed by selecting the BEMC-trigger hadron as one of the decay daughters. We also show that the trigger efficiency can be obtained reliably in simulation and data-driven approaches.

Key words: EMC, hadronic trigger, trigger efficiency

PACS: 29.40.Cs, 29.85.Fj

Email address: xuyichun@mail.ustc.edu.cn (Yichun Xu).

1 Introduction

One of the main physics goals of the Relativistic Heavy Ion Collider (RHIC) with the experiment of the Solenoidal Tracker at RHIC (STAR) [1] in recent (and future) years is to study the properties of the Quark-Gluon-Plasma (QGP) created in the heavy ion collisions [2]. An important probe is to use the identified high- p_T hadrons to study the color charge effect of parton energy loss in heavy ion collisions[3,4,5,6,7,8]. At RHIC, the luminosity is usually much higher than the detector and data acquisition capability. RHIC delivers $p+p$ collision rates of several MHz while the STAR Time Projection Chamber (TPC) readout is around one kHz . Trigger detectors are used to implement an online selection of events of interest to the program. An example of such a detector is the electromagnetic calorimeter (EMC) used to select events with high energy deposit from an electromagnetic shower in the detector. This can enhance the event sample with high energy neutral pions or energetic jets with significant electromagnetic components (π^0 or γ). However, STAR has no hadronic calorimeter to select the final state charged hadrons although those hadrons do leave ionization tracks behind in the TPC or other tracking detectors. To date, charged hadron spectra in $p+p$ and $A+A$ collisions at RHIC have only been obtained using a minimum-bias trigger and their upper reach in p_T is severely limited by rapidly falling statistics at high- p_T from such an all-inclusive trigger. For example, the charged pion spectra are so far only measured at RHIC to $p_T \simeq 10 \text{ GeV}/c$ in $p+p$ collisions, while the π^0 spectra reach $p_T \simeq 20 \text{ GeV}/c$. On the other hand, the STAR EMC contains about one hadronic interaction length of material and can perform online trigger selection of events based on energy deposition in finely segmented towers. Charged hadrons do interact and produce showers with a significant amount of energy in the EMC at a lower efficiency.

In this paper, we present a study of hadronic trigger efficiency from the STAR Barrel EMC (BEMC) [9]. Different BEMC energy thresholds and BEMC patch sizes are used in this study. The inclusive charged hadron spectra are selected from the away-side opposite the struck calorimeter tower (or jet patch). PYTHIA simulations are performed to correct for the trigger effect. In addition to the enhancement of single hadron yields at high momentum, these triggers also allow us to construct resonances and weak-decay particles from their charged hadron daughters by requiring that one of the daughters produce a BEMC signal above the trigger threshold. The trigger effect on resonance and V_0 reconstructions is corrected using the experimental data. This approach avoids a demanding simulation of the details of the detector and trigger performances on the struck EMC tower. These not only extend the measurements of identified hadron spectra to much higher momentum, but also provide crucial consistency checks among different measurements over the same momentum range: π^0 vs π^\pm , K_S^0 vs K^\pm . The current manuscript provides the technical

43 details of the triggers, analyses, correction and systematics while the scientific
44 results have been discussed in Ref. [10].

45 2 Experimental Setup and Data Analysis

46 2.1 Detectors and Datasets

47 The data used for this study were collected with the STAR Experiment in the
48 year 2005 requiring the minimum-bias trigger condition plus energy deposition
49 in the BEMC detector for $p + p$ collisions. For this data, the total BEMC
50 coverage is $0 < \eta < 1$ and $0 < \phi \leq 2\pi \text{ rad}$. Each calorimeter tower covers
51 $\Delta\eta \times \Delta\phi = 0.05 \times 0.05 \text{ rad}$ in pseudo-rapidity (η), and azimuthal angle
52 (ϕ). The online energy deposition triggers utilize either a single BEMC tower
53 (high-tower trigger, HT) or a contiguous $\Delta\eta \times \Delta\phi = 1 \times 1 \text{ rad}$ region (jet
54 patch trigger, JP) of the BEMC [11]. A total of 5.6 million JP events with
55 transverse energy $E_T > 6.4 \text{ GeV}$ are used for π^\pm , K^\pm , and $p(\bar{p})$ analyses.
56 To reduce trigger biases and to avoid the demandingly precise simulation of
57 hadronic showers and the detector trigger response, only away-side particles
58 (at azimuthal angles $90^\circ - 270^\circ$ from the JP trigger) are used in the analyses of
59 the inclusive single charged hadron spectra. The high-tower trigger condition
60 requires the energy of a single calorimeter tower to be at least 2.6 GeV (HT1)
61 or 3.5 GeV (HT2) [12,13]. In total, 5.1 million HT1 and 3.4 million HT2 events
62 were collected from 0.65 pb^{-1} and 2.83 pb^{-1} integrated sampled luminosity of
63 proton beams. These datasets are used for $K_S^0 \rightarrow \pi^+ + \pi^-$, $\bar{\Lambda} \rightarrow \bar{p} + \pi^+$ and
64 $\rho^0 \rightarrow \pi^+ + \pi^-$ reconstruction by requiring that one of the daughter pions or
65 antiproton triggered the high tower.

66 The TPC covers $0 < \phi \leq 2\pi \text{ rad}$ and $|\eta| \leq 1.3$ with up to 45 reconstructed
67 hit points to serve as STAR's main tracking detector. It measures ioniza-
68 tion energy loss (dE/dx) and momentum (via curvature) of tracks in a 0.5
69 T solenoidal magnetic field, which together can provide particle identifica-
70 tion, including along the relativistic rise at high momentum [14]. Topology
71 of the daughter tracks from high- p_T K_S^0 , $\Lambda(\bar{\Lambda})$, ρ^0 , K^* , D^0 and other reso-
72 nances can be reconstructed through their hadronic decay into at least one
73 high- p_T charged hadron. In all of the analyses discussed here, the collision
74 vertex is required to be within 100 cm of the TPC center. More details of
75 hadron identification at high- p_T [15,16,17] and topological V0 reconstruction
76 of weak-decay particles [8] can be found in the references.

78 In addition to the required azimuthal angle between the track and the JP
 79 trigger center to be $|\Delta\phi| \geq \pi/2$ rad in the analyses of charged hadron spectra
 80 of π^\pm , K^\pm and $p(\bar{p})$, the TPC tracks are selected based on: $|\eta| < 0.5$, distance
 81 of closest approach of the track helix projection to the collision vertex to be
 82 within 1.0 cm, number of TPC hits to be at least 25 and at least 52% of the
 83 maximum possible hits, and the TPC hits involved in the dE/dx calculation
 84 after truncation to be at least 15. In each p_T bin, the normalized dE/dx ,
 85 $n\sigma_\pi$ [15,16,17,18] distributions of positively and negatively charged particles
 86 are histogrammed. The detailed method of calibration and extraction of raw
 87 counts of the individual identified hadrons from the same data sample has
 88 been previously published [15].

89 The JP triggers enhance the statistics greatly, but also require additional
 90 corrections with normalization and momentum-dependent efficiency. Figure 1
 91 shows raw charged pion spectra in the BEMC-trigger events compared to the
 92 published results (squares) in minimum-bias events [4]. This demonstrates
 93 that charged pions in the BEMC-trigger data sample are enriched by an order
 94 of magnitude at low p_T ($\simeq 3$ GeV/c) and by three orders of magnitude at
 95 high p_T ($\gtrsim 10$ GeV/c). To correct for this trigger effect, PYTHIA events are
 96 embedded into the STAR detector geometry in GEANT, which can simulate
 97 the realistic response of the STAR detector. The Monte Carlo simulation is
 98 based on PYTHIA version 6.205 [19] with CDF Tune A settings [20]. The
 99 same simulation setup has been used in other jet related analyses [11]. In
 100 order to fully cover the falling power-law spectrum in p_T of reconstructed
 101 particles with sufficient statistics, the data samples are generated according to
 102 the initial parton p_T (in units of GeV/c) intervals (0,2), (2,3), (3,4), (4,5), (5,7),
 103 (7,9), (9,11), (11,15), (15,25), (25,35) and (>35). The spectra are weighted by
 104 the cross-sections in each parton p_T range. Table 1 shows the absolute cross-
 105 sections (σ_i) for $p + p$ collisions which generate the partons at each given p_T
 106 interval and the number of events (N_i) going through the full simulation chain.
 107 The obtained hadron spectra have to be weighted with the factor (proportional
 108 to σ_i/N_i) according to their originating partons.

109 The simulation includes detector response to the signal, electronic readout,
 110 and detector and background noise when particles propagate through the de-
 111 tector. The BEMC-trigger configuration and thresholds are then applied in
 112 the same way as in the real events from experiment. The resulting charged
 113 pion spectra from these simulations are shown on the left panel in Figure 1
 114 for the minimum-bias-trigger and the BEMC-trigger events. The enhancement
 115 of charged pions can be calculated by dividing the BEMC-trigger spectra by
 116 the minimum-bias-trigger spectra from these PYTHIA simulations. The right
 117 panel in Figure 1 shows the enhancement factor as a function of transverse

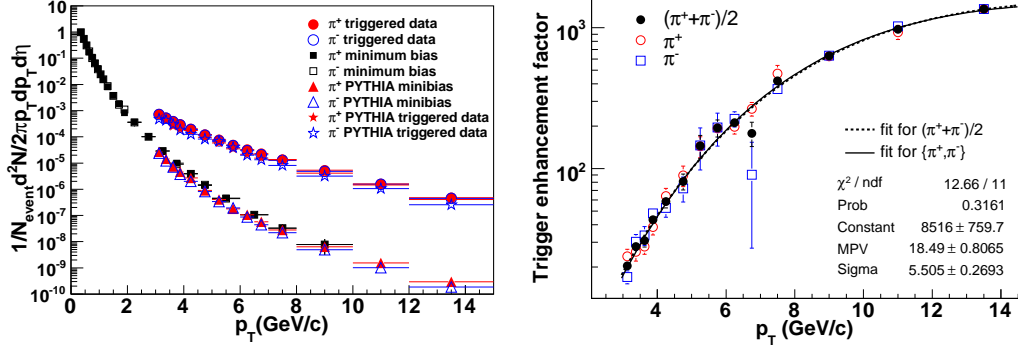


Fig. 1. The left panel shows pion spectra in minimum-bias and BEMC-trigger events from both measurements and the PYTHIA+GEANT simulation. Triggered enhancement from the simulations versus p_T distribution is shown on the right panel.

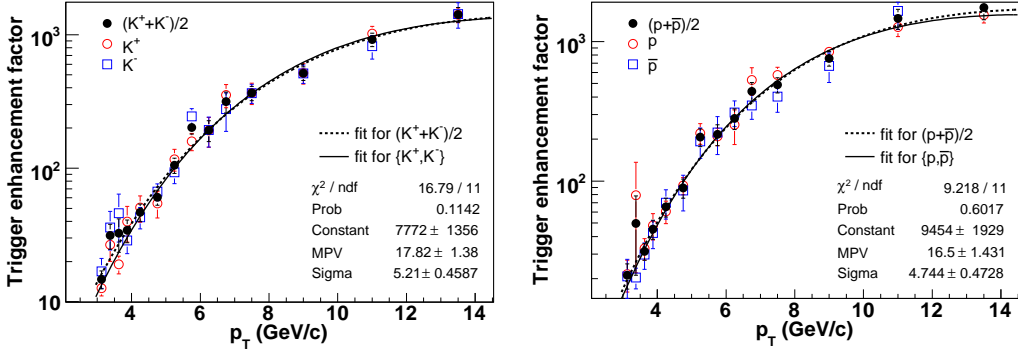


Fig. 2. Trigger enhancement factor distribution for kaon and proton are shown on the left and right panels respectively.

118 momentum. Similarly, the trigger enhancement factors for kaon and proton
 119 are calculated and presented in the left and right panels in Figure 2. These
 120 factors are then applied to the raw spectra to obtain the inclusive invariant
 121 differential cross-section of the charged hadrons in $p+p$ collisions as presented
 122 in Ref. [10].

123 Since the correction for the JP trigger relies entirely on the PYTHIA event
 124 generator through the STAR detector simulation chain, concerns were raised
 125 whether the PYTHIA event generator simulates the jets and underlying event
 126 structure correctly and whether the detector simulation reproduces the JP
 127 trigger truthfully. To quantify this, several triggers with different jet-patch
 128 and high-tower energy thresholds have been used to study the systematic
 129 differences among the spectra after all the corrections have been applied, pro-
 130 viding an estimate of the systematic uncertainty due to these effects. These
 131 are the largest contributions to the overall systematic uncertainties, especially
 132 at intermediate p_T [7,10].

133 Studies have shown that the underlying event structure [21] and the jet spec-

Table 1

Parton p_T interval, the corresponding absolute cross-section and the number of events generated in PYTHIA through the STAR simulation and reconstruction chain.

parton p_T (GeV/c)	Cross-section (mb)	Number of events
(0,2)	18.2	339083
(2,3)	8.11	507996
(3,4)	1.30	400629
(4,5)	0.314	600980
(5,7)	1.36e-1	431000
(7,9)	2.31e-2	412000
(9,11)	5.51e-3	416000
(11,15)	2.22e-3	416000
(15,25)	3.89e-4	408000
(25,35)	1.02e-5	380000
(> 35)	5.30e-7	100000

134 tra [11] match well between data and PYTHIA. The results also show that the
 135 averaged π^\pm spectrum obtained from this method are consistent with the π^0
 136 spectra from both STAR [13] and PHENIX [22] to within 10%. The π^0 spectra
 137 were obtained with a completely different trigger scheme: one of the photons
 138 from π^0 decay has to be reconstructed from the BEMC high-tower, which trig-
 139 gers the event. Therefore, the π^0 trigger is not affected by the event structure
 140 but depends on the simulation of the photon response and trigger efficiency. In
 141 the following sections, we describe a similar method to reconstruct resonances
 142 and V0 decays by using a BEMC high-tower as a hadronic trigger on one of
 143 the charged hadronic daughters. The trigger efficiency of the daughter hadrons
 144 is obtained directly from dividing the raw observed spectra of π^\pm and $p(\bar{p})$ by
 145 their respective invariant spectra. Powerful consistency checks on trigger bias
 146 and $K^\pm dE/dx$ uncertainty are possible by comparing the K^\pm spectra from
 147 jet away-side triggers and published minimum-bias-trigger results [8] with the
 148 invariant spectra of $K_S^0 \rightarrow \pi^+ + \pi^-$ from our hadronic trigger.

149 2.3 Trigger enhancement and efficiency for showering hadrons

150 In this section, we provide the detailed procedure of obtaining the π^\pm and
 151 $p(\bar{p})$ trigger efficiencies when either is associated with the high-tower that
 152 passes the online trigger threshold, where these are daughters from resonance

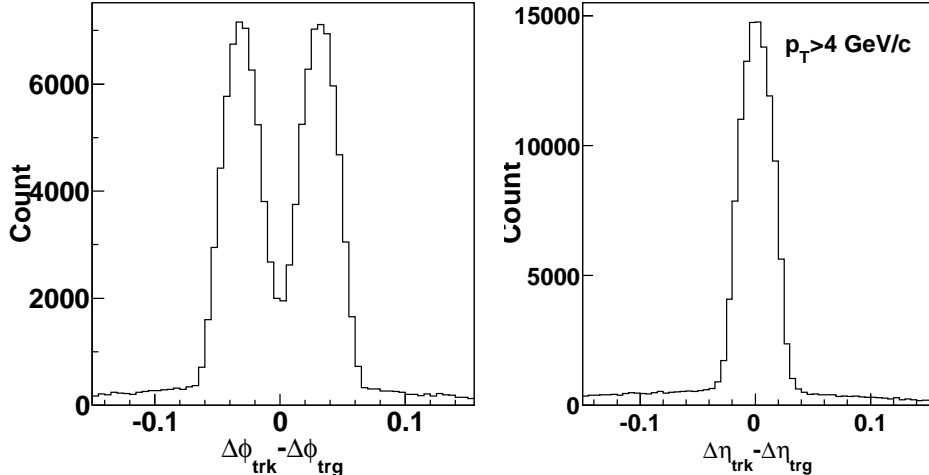


Fig. 3. The $\Delta\phi$ and $\Delta\eta$ between tracks and BEMC triggered towers. We note that the splitting into two peaks in $\Delta\phi$ (i.e. in the bending plane) is due to the fact that the TPC track helices are projected to the BEMC surface while in reality the hadronic showers are on average deep within the BEMC.

153 ($\rho^0 \rightarrow \pi^+ + \pi^-$) or V0 ($K_S^0 \rightarrow \pi^+ + \pi^-$, $\Lambda(\bar{\Lambda}) \rightarrow p(\bar{p}) + \pi^{-(+)}$) decays. In
 154 offline analysis, a track reconstructed in the TPC is projected to the surface
 155 of the BEMC and associated with a shower reconstructed from the BEMC
 156 tower energies. The distances between the center of the triggered tower and
 157 the track projections are shown in Figure 3. We require $|\Delta\phi| < 0.075$ rad and
 158 $|\Delta\eta| < 0.075$ for matched tracks. Projecting the backgrounds under the peaks,
 159 we find that these cuts include $\sim 3\%$ of accidental coincidences, most of which
 160 will be further reduced by additional cuts.

161 Although hadronic interactions in an electromagnetic calorimeter develop show-
 162 ers for which much of the energy escapes the detector, a significant fraction
 163 of hadrons leave a sizable captured energy deposition. Figure 4 shows the cor-
 164 relation between energy deposited in the triggered tower and momentum of
 165 the matched track. The particles are selected between two cuts (shown in the
 166 figure) on $E \leq 2 \times p$, to remove accidental coincidences with electromagnetic
 167 showers, and $E > 2$ GeV, to reject minimum ionizing particles and other low
 168 energy background coincidences. This provides a dataset with a wide momen-
 169 tum range for further particle identification.

170 The normalized dE/dx , $n\sigma_\pi$ [15,16,17,18] distributions at $3.25 < p_T < 3.50$
 171 GeV/c, offset by +6 for positive particles and -6 for negative particles, are
 172 shown in Figure 5. The peaks of triggered electrons and positrons are clearly
 173 separated from charged hadrons. Statistics of charged pions and anti-protons
 174 are significantly enhanced in comparison to the distributions for minimum-
 175 bias-trigger data [15]. The yield of triggered anti-protons is much larger than
 176 that of protons because they annihilate with the material in the BEMC and
 177 deposit an additional ~ 2 GeV extra energy.

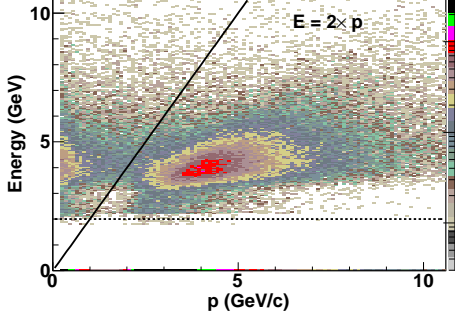


Fig. 4. Energy of triggered towers versus momentum of matched tracks. Only tracks with $p_T > 3$ GeV/c are used in the analyses.

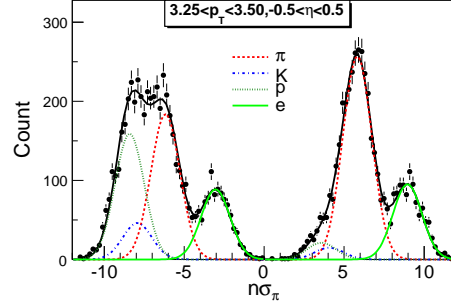


Fig. 5. Normalized dE/dx distributions at $3.25 < p_T < 3.50$ GeV/c.

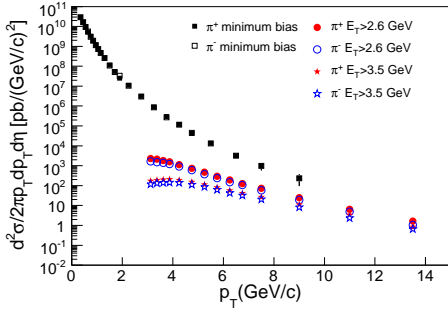


Fig. 6. pion p_T spectra from minimum-bias events and BEMC-trigger events.

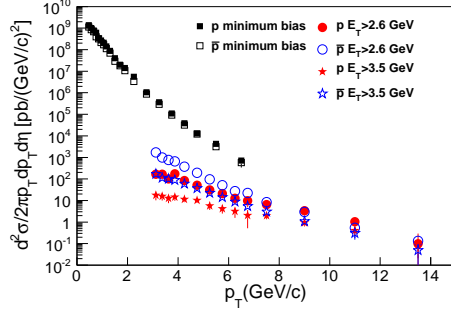


Fig. 7. proton p_T spectra from minimum-bias events and BEMC-trigger events.

178 Efficiencies can be derived by dividing the raw p_T spectra in the BEMC-
 179 trigger events by the inclusive invariant spectra obtained previously (shown
 180 in Figure 6 and Figure 7 respectively), and these efficiencies for pions and
 181 (anti-)protons are shown in Figure 8 and Figure 9. Although the efficiency is
 182 not as high as a pure electromagnetic shower, the trigger enhancement is quite
 183 high. Taking pion efficiency as an example, at $p_T = 5$ GeV/c, the triggered pion
 184 efficiency in HT1 is $\sim 2\%$, and therefore the 5.1 million HT1 events (from 0.65
 185 pb^{-1} sampled luminosity) are equivalent to luminosity $(0.65 pb^{-1}) \times \sigma_{pp}^{NSD} (30$
 186 $mb) \times [\text{trigger efficiency}](2\%) / [\text{tracking efficiency}](90\%) = \sim 450$ million minimum-
 187 bias-trigger (non-single diffractive [NSD]) events. This means a factor of ~ 100
 188 times more statistics for charged pions at this p_T in this data sample than in
 189 the previously published minimum-bias-trigger sample [3]. At higher p_T , the
 190 trigger efficiency and the minimum-bias event equivalents are much higher.
 191 The details can be found in Tables 2 and 3. Therefore, the BEMC-trigger
 192 data samples significantly enhance the available statistics of the particles at
 193 high p_T .

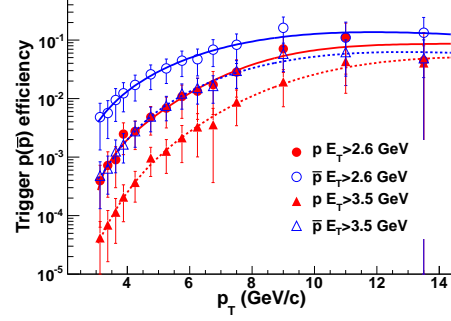
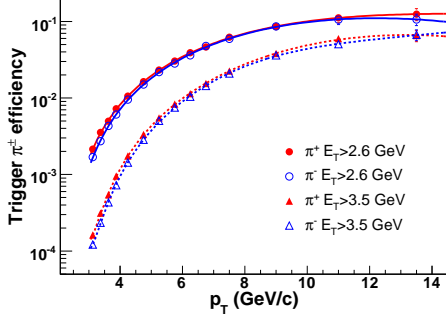


Fig. 8. Trigger efficiency and tracking efficiency of pion from BEMC-trigger events.

Fig. 9. Trigger efficiency and tracking efficiency of proton and anti-proton from BEMC-trigger events.

Table 2

The number of equivalent minimum-bias events (N_{eq}) for charged pion at given p_T bin from 5.1 million HT1 and 3.4 million HT2 events respectively.

p_T	$N_{eq}(\pi^+)$ HT1	$N_{eq}(\pi^-)$ HT1	$N_{eq}(\pi^+)$ HT2	$N_{eq}(\pi^-)$ HT2
3.125	4.66e+07	3.61e+07	1.53e+07	1.16e+07
3.375	7.56e+07	6.11e+07	2.89e+07	2.15e+07
3.625	1.11e+08	9.28e+07	5.29e+07	4.10e+07
3.875	1.53e+08	1.32e+08	8.81e+07	7.08e+07
4.25	2.29e+08	2.03e+08	1.64e+08	1.37e+08
4.75	3.52e+08	3.21e+08	3.11e+08	2.68e+08
5.25	4.97e+08	4.64e+08	5.15e+08	4.54e+08
5.75	6.62e+08	6.30e+08	7.77e+08	6.97e+08
6.25	8.41e+08	8.11e+08	1.10e+09	9.98e+08
6.75	1.03e+09	1.00e+09	1.47e+09	1.35e+09
7.5	1.32e+09	1.30e+09	2.13e+09	1.97e+09
9	1.86e+09	1.83e+09	3.59e+09	3.38e+09
11	2.38e+09	2.26e+09	5.33e+09	5.02e+09
13.5	2.73e+09	2.32e+09	6.38e+09	5.92e+09

194 2.4 Resonance and V0 reconstruction

195 The BEMC-trigger data sample not only increases the stable hadron yields to
 196 tape, but also provides those high-statistic stable hadrons for the resonance
 197 and V0 reconstructions. To reconstruct K_S^0 or $\Lambda(\bar{\Lambda})$ via their dominant weak
 198 decay channels, $K_S^0 \rightarrow \pi^+ + \pi^-$, $\Lambda(\bar{\Lambda}) \rightarrow p(\bar{p}) + \pi^{-(+)}$, we look for at least

Table 3

The number of equivalent minimum-bias events (N_{eq}) for proton and anti-proton at given p_T bin from 5.1 million HT1 and 3.4 million HT2 events respectively.

p_T	$N_{eq}(p)$ HT1	$N_{eq}(\bar{p})$ HT1	$N_{eq}(p)$ HT2	$N_{eq}(\bar{p})$ HT2
3.125	7.88e+06	9.66e+07	3.75e+06	4.41e+07
3.375	1.59e+07	1.41e+08	6.79e+06	6.70e+07
3.625	2.53e+07	1.94e+08	1.17e+07	1.04e+08
3.875	3.66e+07	2.55e+08	1.90e+07	1.56e+08
4.25	5.77e+07	3.62e+08	3.53e+07	2.63e+08
4.75	9.61e+07	5.32e+08	7.01e+07	4.63e+08
5.25	1.50e+08	7.30e+08	1.25e+08	7.29e+08
5.75	2.24e+08	9.53e+08	2.06e+08	1.06e+09
6.25	3.19e+08	1.19e+09	3.18e+08	1.45e+09
6.75	4.38e+08	1.44e+09	4.69e+08	1.89e+09
7.5	6.56e+08	1.81e+09	7.77e+08	2.62e+09
9	1.16e+09	2.46e+09	1.68e+09	4.09e+09
11	1.66e+09	2.92e+09	3.20e+09	5.50e+09
13.5	1.86e+09	2.85e+09	4.53e+09	5.86e+09

199 one of the decay daughters to be the particle firing the BEMC trigger. This
 200 procedure has also been used in the cross section measurement reported in
 201 Ref. [8,23].

202 The reconstructed event vertex is required to be along the beam axis and
 203 within 100 *cm* of the TPC center to ensure uniform tracking efficiency. A search
 204 is made in each event to find a (anti-)proton and pion tracks of the opposite
 205 curvature. The tracks are then paired to form a K_S^0 or $\Lambda(\bar{\Lambda})$ candidate and
 206 topological selections are applied to reduce backgrounds. Figures 10 and 11
 207 show invariant mass distributions of the triggered K_S^0 and $\Lambda(\bar{\Lambda})$ at high p_T with
 208 only 3.4 million HT2 BEMC-trigger events, while 10 million minimum-bias
 209 events can only reach 5 *GeV/c* due to limited statistics [8].

210 To obtain the invariant spectra, we need to apply the correction factors due
 211 to the efficiencies of trigger, tracking and topological cuts. The correction
 212 is divided into two factors: kinematic efficiency and topological efficiency. We
 213 define the kinematic efficiency to include the effects of the BEMC response and
 214 trigger, the TPC tracking efficiency, and the acceptance due to kinematics. The
 215 topological efficiency includes the effects due to the topological requirements
 216 in V0 reconstruction and is found to be p_T independent at 92% for K_S^0 (the

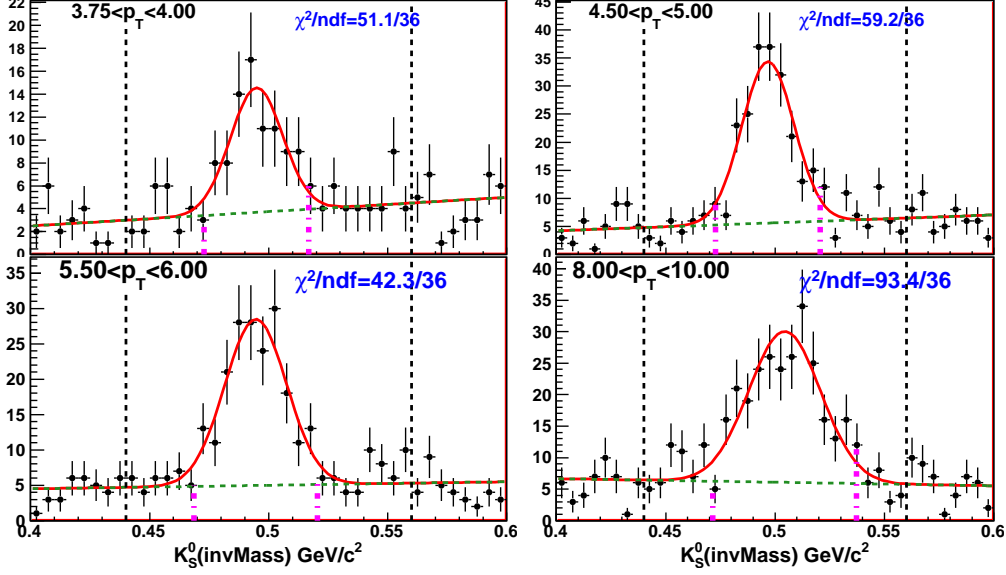


Fig. 10. Invariant mass of K_S^0 at several high p_T bins.

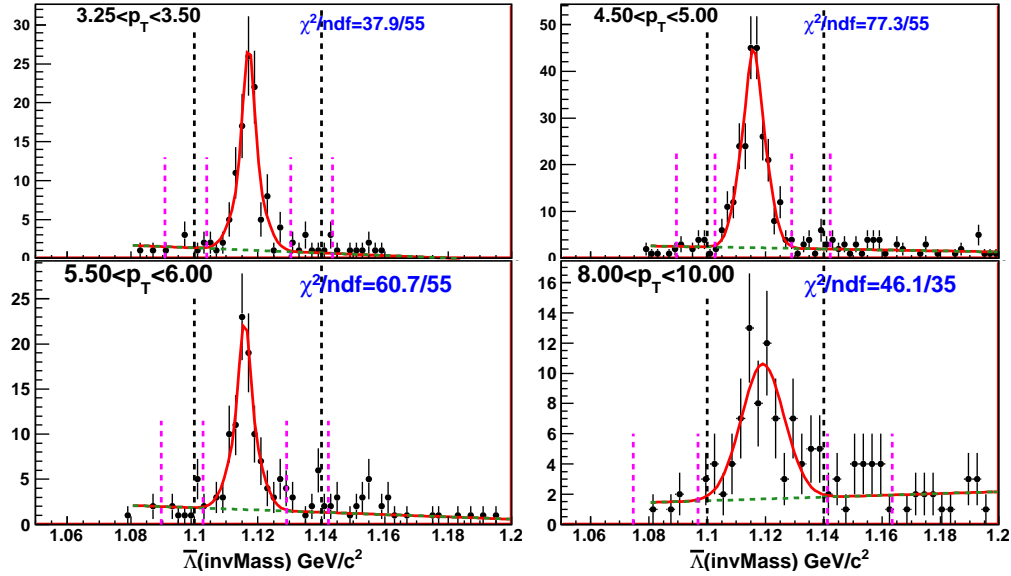


Fig. 11. Invariant mass of $\bar{\Lambda}$ at several high p_T bins.

217 topological efficiencies of $\Lambda(\bar{\Lambda})$ are still under study as of this writing) [8].
 218 Figures 12, 13 and 14 are the kinematic efficiencies as a function of p_T for the
 219 reconstruction of parent particles K_S^0 , $\bar{\Lambda}$ and ρ^0 , respectively.

220 Resonances ($\rho^0 \rightarrow \pi^+ + \pi^-$, $K^* \rightarrow K^\mp + \pi^\pm$ etc.) can be reconstructed in
 221 a similar fashion. Since ρ^0 decays strongly with a lifetime of about $1 \text{ fm}/c$,
 222 reconstruction from its pion daughter pairs is made without the displaced de-
 223 cay topological constraints used in V0 reconstruction. The invariant masses
 224 of unlike-sign ($\pi^+ + \pi^-$) and like-sign ($\pi^\pm + \pi^\pm$) pion pairs are calculated and
 225 shown in Figure 15. Panel (a) from this figure is for the invariant distribu-

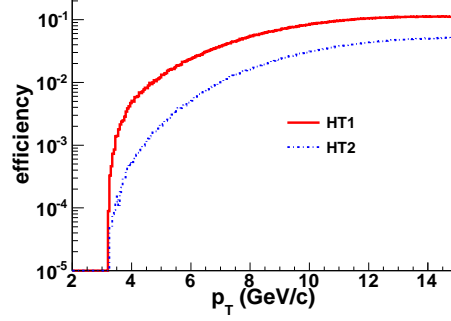
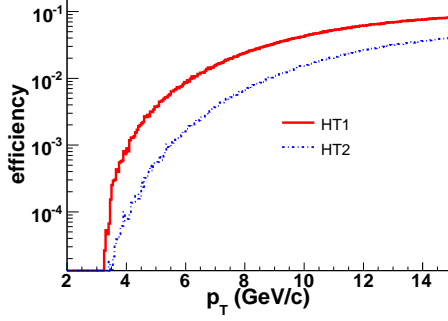


Fig. 12. Kinematic efficiency of K_S^0 vs. p_T . Fig. 13. Kinematic efficiency of $\bar{\Lambda}$ vs. p_T .

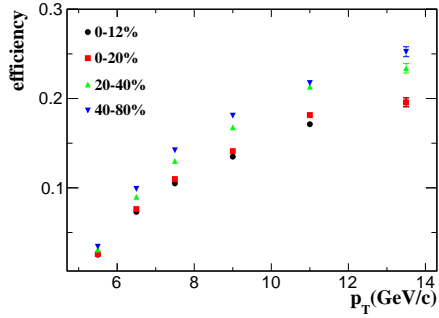


Fig. 14. Kinematic efficiency of ρ^0 vs. p_T .

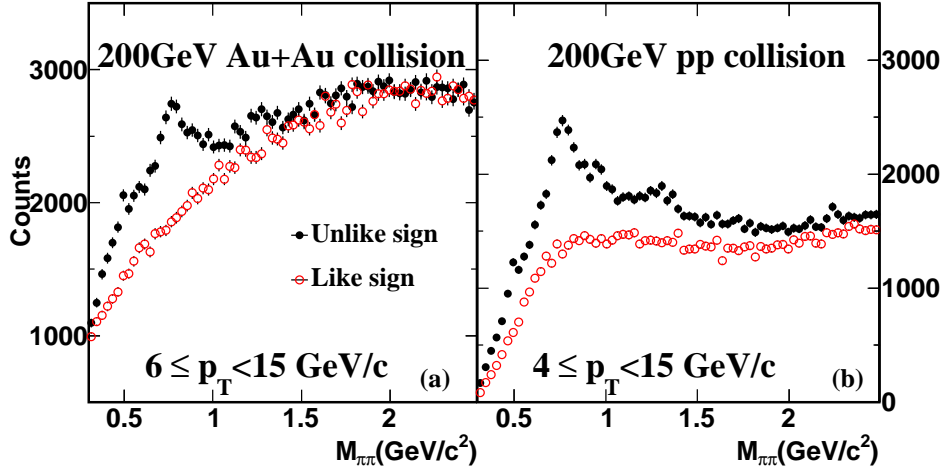


Fig. 15. Invariant mass distributions of the unlike-sign pairs $\pi^+ + \pi^-$ and like-sign pairs $\pi^\pm + \pi^\pm$ around the ρ^0 mass. Panels (a) and (b) show the distributions from Au+Au and $p + p$ collisions respectively.

226 tions in Au+Au collisions while panel (b) is for $p + p$ collisions. The like-sign
 227 pairs represent the random combinatoric background and the excess above this
 228 background distribution in the unlike-sign is attributable to particle decays
 229 (ρ^0 , ω , f_0 , and f_2). Figure 16 shows the $\pi^+ + \pi^-$ invariant mass distribution
 230 after like-sign background subtraction.

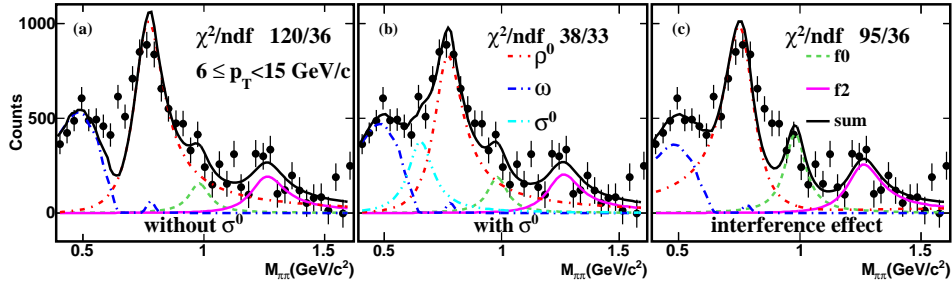


Fig. 16. Invariant mass distribution of $\pi^+ + \pi^-$ around the ρ^0 mass. The three panels show fits for (a) a four-species cocktail, (b) cocktail with additional σ_0 , and (c) cocktail with an additional interference term.

231 For the line shape of $\rho^0 \rightarrow \pi^+ + \pi^-$, the procedure and formula from a low- p_T
 232 study are used with the ρ^0 mass at $775 \text{ MeV}/c^2$ and Breit-Wigner width of
 233 $155 \text{ MeV}/c^2$ [24]. As with that study, a four-species cocktail describes the
 234 data quite well except that it under-describes data at invariant mass around
 235 $600 \text{ MeV}/c^2$. This is clearly visible in Figure 16(a). To investigate the possi-
 236 ble missing components of the cocktail and how they impact the extracted
 237 ρ^0 yields, we perform two additional studies by adding a σ^0 to the cock-
 238 tail and by adding an interference term between $\rho^0 \rightarrow \pi^+ + \pi^-$ and direct
 239 $\pi^+ + \pi^- \rightarrow \pi^+ + \pi^-$ scattering. Inclusion of the possible σ^0 particle [25] (mass
 240 at $\sim 600 \text{ MeV}/c^2$ and Breit-Wigner width scanning from 100 to $500 \text{ MeV}/c^2$)
 241 results in 20% lower ρ^0 yields and improves the χ^2 per degree of freedom
 242 (χ^2/NDF) from 120/36 to 38/33, a factor of nearly 3 improvement. This fit
 243 is shown in Figure 16(b) and is used to obtain the default ρ^0 yields, where the
 244 σ^0/ρ^0 ratio is about 25% independent of p_T . An additional systematic check
 245 is performed using the modified Soeding parametrization for a possible inter-
 246 ference effect on the ρ^0 line shape [26]. This parametrization and the relative
 247 amplitudes of its two interference terms are determined from clear signals and
 248 well-defined processes in ultra-peripheral Au+Au collisions. Both the result-
 249 ing χ^2/NDF and the ρ^0 yield fall between the other two fits. Figure 16(c)
 250 shows that including the interference over-corrects the high-mass tail of the
 251 ρ^0 spectral distribution and therefore under-predicts the data.

252 3 Summary

253 An electromagnetic calorimeter (the STAR BEMC) is leveraged to enhance
 254 the event sample containing charged hadrons at high transverse momentum,
 255 utilizing the STAR TPC for momentum reconstruction and species identifi-
 256 cation through dE/dx . The away-side hadrons opposite triggered jet patches
 257 (high collective energy in a group of BEMC towers) are used to determine
 258 inclusive spectra of identified stable charged hadrons at high p_T . Events trig-
 259 gered by high energy in a single BEMC tower are used to find hadronic shower

260 candidates by matching these towers to high p_T TPC tracks. These tracks are
 261 then paired with other charged hadrons to reconstruct K_S^0 and $\Lambda(\bar{\Lambda})$ through
 262 their dominant decay channels: $K_S^0 \rightarrow \pi^+ + \pi^-$ and $\Lambda(\bar{\Lambda}) \rightarrow p(\bar{p}) + \pi^{-(+)}$.
 263 With this method, spectra of the identified charged hadrons, K_S^0 and $\Lambda(\bar{\Lambda})$
 264 have been extended to higher p_T (~ 12 GeV/c) under the existing detector
 265 and RHIC luminosity capabilities [8]. This method is also used to extend the
 266 p_T reach for efficiently reconstructing strongly decaying particles, such as ρ^0
 267 and K^* .

268 Acknowledgments

269 We thank the STAR Collaboration, the RHIC Operations Group and RCF
 270 at BNL, and the NERSC Center at LBNL for their support. This work was
 271 supported in part by the Offices of NP and HEP within the U.S. DOE Office of
 272 Science; Authors Yichun Xu and Zebo Tang are supported by National Natural
 273 Science Foundation of China under Grant No. 11005103 and No. 11005104,
 274 and Hongyu Da and Xiangli Cui are supported by the Knowledge Innova-
 275 tion Program of the Chinese Academy of Sciences, Grant No. kjc2-yw-a14,
 276 NSFC(10620120286, 10620120285).

277 References

- 278 [1] K. H. Ackermann *et al.* [STAR Collaboration], Nucl. Instrum. Meth. A **499**,
 279 624 (2003).
- 280 [2] J. Adams *et al.* [STAR Collaboration], Nucl. Phys. A **757**, 102 (2005)
 281 [arXiv:nucl-ex/0501009].
- 282 [3] L. Ruan [STAR Collaboration], J. Phys. G **34**,
 283 S199 (2007) [arXiv:nucl-ex/0701070]; J. Adams *et al.* [STAR Collaboration],
 284 Phys. Lett. B **616**, 8 (2005) [arXiv:nucl-ex/0309012]; B. I. Abelev *et al.* [STAR
 285 Collaboration], Phys. Lett. B **655**, 104 (2007) [arXiv:nucl-ex/0703040]; B.I.
 286 Abelev *et al.* [STAR Collaboration], Phys. Rev. Lett. **97**, 152301 (2006).
- 287 [4] J. Adams *et al.* [STAR Collaboration], Phys. Lett. B **637**, 161 (2006)
 288 [arXiv:nucl-ex/0601033].
- 289 [5] Yichun Xu (for STAR Collaboration) J. Phys. G: Nucl. Part. Phys. **37** (2010)
 290 094059
- 291 [6] Yichun Xu (for STAR Collaboration) Eur. Phys. J. C (2009) **62**: 187
- 292 [7] Yichun Xu (for STAR Collaboration) Nuclear Physics A **830** (2009) 701; Yichun
 293 Xu, PH.D. thesis, USTC 2009.

- 294 [8] B. I. Abelev *et al.* [STAR Collaboration], Phys. Rev. C 75, 064901 (2007).
- 295 [9] M. Beddo *et al.* [STAR Collaboration], Nucl. Instrum. Meth. A **499** (2003) 725.
- 296 [10] STAR Collaboration (G. Agakishiev et al.), e-Print: arXiv:1110.0579.
- 297 [11] B. I. Abelev *et al.*, Phys. Rev. D 79, 112006 (2009); B. I. Abelev *et al.*, Phys.
298 Rev. Lett. 100, 232003 (2008); B. I. Abelev *et al.*, Phys. Rev. Lett. 97, 252001
299 (2006).
- 300 [12] F. S. Bieser *et al.*, Nucl. Instrum. Meth. A **499**, 766 (2003).
- 301 [13] B.I. Abelev et al., (STAR Collaboration) Phys. Rev. C 81 (2010) 64904
- 302 [14] M. Anderson *et al.*, Nucl. Instrum. Meth. A **499**, 679 (2003)
303 [arXiv:nucl-ex/0205014].
- 304 [15] Yichun Xu et al., Nuclear Instruments and Methods in Physics Research
305 A614(2010)28.
- 306 [16] M. Shao *et al.*, Nucl. Instrum. Meth. A **558**, 419 (2006) [arXiv:nucl-ex/0505026].
- 307 [17] H. Bichsel, Nucl. Instrum. Meth. A **562** (2006) 154.
- 308 [18] M. Aguilar-Benitez *et al.*, Z. Phys. C **50**, 405 (1991).
- 309 [19] T. Sjostrand *et al.*, Comput. Phys. Commun. 135, 238 (2001)
- 310 [20] R. D. Field *et al.*, arXiv:hep-ph/0510198
- 311 [21] H. Caines [STAR Collaboration], Nucl. Phys. **A855**, 376-379 (2011).
- 312 [22] A. Adare *et al.* [PHENIX Collaboration], Phys. Rev. Lett. **101** (2008) 232301
313 [arXiv:0801.4020 [nucl-ex]].
- 314 [23] Yan Lu, PH.D. Thesis, Central China Normal University Wuhan, 2005.
- 315 [24] J. Adams *et al.*, Phys. Rev. Lett. **92** (092301) 2004; B.I. Abelev *et al.*, Phys.
316 Rev. C **78**, 044906 (2008).
- 317 [25] R. Garcia-Martin *et al.*, Phys. Rev. Lett. **107** (072001) 2011.
- 318 [26] B.I. Abelev *et al.*, Phys. Rev. C **77** (034910) 2008.